Malaysian Journal of Chemistry, 2024, Vol. 26(5), 442-454
(Special Issue: *4th IKMPB Online Symposium 2024 - Development of Chemistry to Accomplish a Sustainable World*)

Formulation and Characterization of Celecoxib-loaded Fractionated Medium Chain Triglycerides Oil Based Nanoemulgel

Nuriana Munirah Hairul[1], Nor Khaizan Anuar[1], Mohd Hanif Zulfakar[2], Norazlinaliza Salim[3,4]* and Salizatul Ilyana Ibrahim[1,5]*

[1]Faculty of Pharmacy, Universiti Teknologi MARA, Cawangan Selangor, Kampus Puncak Alam, 42300 Puncak Alam, Selangor, Malaysia
[2]Centre for Drug Delivery Technology & Vaccine, Faculty of Pharmacy, Universiti Kebangsaan Malaysia, 50300, Kuala Lumpur, Malaysia
[3]Centre for Foundation Studies in Science, Universiti Putra Malaysia, 43400, UPM Serdang, Selangor, Malaysia
[4]Halal Products Research Institute, Universiti Putra Malaysia, 43400 UPM, Serdang, Selangor, Malaysia,
[5]Centre of Foundation Studies, Universiti Teknologi MARA, Cawangan Selangor, Kampus Dengkil, 43800 Dengkil, Selangor, Malaysia
*Corresponding author (e-mail: saliza2910@uitm.edu.my; azlinalizas@upm.edu.my)

Celecoxib (CXB) is a lipophilic drug with limited solubility in water and reduced oral bioavailability. Nanoemulgel (NEG) is a promising transdermal delivery system that improves the solubility and bioavailability of poorly water-soluble drugs compared to oral administration. Therefore, this study aimed to develop and characterize a transdermal NEG formulation for CXB, utilizing fractionated medium-chain triglycerides (FMCTs) oils as carrier oils. FMCTs oils, derived from palm kernel oil (*Elaeis guineensis*), are known for their ability to enhance the solubility of lipophilic drugs, making them an appealing choice for this application. The study began by selecting carrier oils - caprylic capric triglyceride (MCT) and a blend with palm kernel olein (PKOlein) based on solubility tests. Phase diagrams were constructed to determine the optimal concentrations for formulating the nanoemulsion (NE). Various NE formulations were prepared using the low-energy emulsification method, followed by formulating corresponding nanoemulgel (NEG) by incorporating Carbopol 940 in varying concentrations. The developed NEs and NEG exhibited the droplet size range between 26.75 and 55.87 nm with the zeta potential values within -22.47 to -38.83 mV and the PDI values less than 0.5, whereas the morphology showed a well-identified spherical particle. Two formulations named NEG-F14 0.5% and NEG-F17 0.5% were selected for further study on the drug content, EE% and in-vitro drug release. Results showed that NEG-F17 0.5% had a higher drug content (97.54%) with 83.39% of EE when compared with NEG-F15 0.5%. The drug release study shows that NEG-F17 0.5% was remarkably higher as compared to NEG-F14 0.5%, due to the presence of PKOlein in nanoemulsion which improve the solubility, decrease particle size, thus increasing the penetration of CXB. These findings collectively suggest that the developed NEs and NEGs offered desirable attributes for their potential in transdermal drug delivery.

Keywords: Celecoxib; lipophilic drug; nanoemulgel; fractionated medium-chain triglycerides oils

Received: January 2024; Accepted: July 2024

In recent years, the transdermal drug delivery system (TDDS) has become an important alternative to other dosage forms due to its non-invasiveness and patient compliance resulting from the ease of application. Additionally, this route also has the advantages of sustained drug action, dose flexibility, reduced side effects, and the ability to bypass hepatic first-pass metabolism [1]. This approach involves the topical application of drug formulation with a certain dosage onto the skin. However, TTDS is limited primarily due to the barrier posed by the outermost layer of skin measuring 10 to 20 µm thick known as stratum corneum (SC) which eventually causes a hindrance for lipophilic drug penetration and successful absorption into systemic blood circulation.

Various nanocarriers have been developed and investigated as potentially useful TDDS. Nanoemulsions (NEs) have become an important nanocarrier used in TDDS to enhance the solubility of lipophilic drugs which can increase both their permeability and bioavailability by improving topical absorption [2]. NEs are thermodynamically stable transparent or translucent systems formed by a mixture of oil phase, surfactant, co-surfactant, and aqueous phase having small droplet sizes ranging from 20 to 200 nm, which eventually could increase skin permeation rate [3]. Moreover, the oils used in the NEs formulation help to solubilize the lipophilic drug and have the potential to increase skin permeability. However, the low viscosity of NEs restrict the application in transdermal

†Paper presented at the 4th IKMPB Online Symposium 2024 – Development of Chemistry to Accomplish a Sustainable World

delivery due to low contact time on the surface of the skin. Therefore, researchers converted NE, either water-in-oil (W/O) or oil-in-water (O/W) into nanoemulgel (NEG) with the addition of gelling agents to achieve a suitable viscosity for topical application. NEGs have overcome the limitation of NE in terms of low viscosity into higher viscosity, good stability, non-greasy, good spreadability, pleasant appearance and ease of removal, and reduced skin irritation [4].

Medium-chain triglycerides (MCTs), namely medium-chain fatty acids (MCFAs) consisting of carbon chain lengths from 6 to 12, are naturally present in various sources that include a palm kernel oil species known as *Elaeis guineensis*. MCTs are harmless and often employed as functional oil in pharmaceutical formulations due to their ability to enhance drug penetration through the skin and excellent solubilizing potential [5]. According to Anand et al. [6], the major composition of MCTs is that they can act as a natural skin permeation enhancer by disorganizing the lipid structure of the SC to facilitate drug penetration and permeation. In this study, fractionated medium chain triglycerides (FMCTs) oil was used as oil phase in NE formulations consisting of PKO and PKOlein (produced through fractionation process) as well as MCT with the commercial name IMEX MCT 60:40 (produced through fractionation and enzymatic esterification process) and all are considered to have higher MCFAs composition [7, 8].

Celecoxib (CXB), a selective cyclo-oxygenase-2 (COX-2) inhibitor of non-steroidal anti-inflammatory drugs (NSAIDs) is known to relieve pain and swelling, reduce inflammation, and is widely used for the long-term treatment of chronic diseases such as rheumatoid arthritis, osteoarthritis, and lupus [9]. CXB is a lipophilic NSAID with a log P of 3.5 and belongs to the biopharmaceutics classification system (BCS) class II because of its low aqueous solubility and high permeability [10, 11]. The low aqueous solubility of the drug can limit the dissolution rate and absorption in the gastrointestinal tract which leads to poor oral bioavailability [12].

As lipophilic CXB has low aqueous solubility, it is selected as a model drug for the current study to determine the solubilizing potential and physicochemical properties using NEG as transdermal nano-vehicle system especially its component, the oil phase and surfactants (FMCTs oils and non-ionic surfactant, respectively) are expected to act as permeation enhancers for better permeation potential through the skin.

EXPERIMENTAL

Chemicals and Materials

CXB with >98% purity, polyoxyethylene sorbitan monooleate (Tween 80), polyoxyethylene sorbitan trioleate (Tween 85), sorbitan monooleate (Span 80), sorbitan monolaurate (Span 20) and Carbopol 940 were procured from Sigma-Aldrich, USA. Meanwhile, palm kernel oil (PKO), palm kernel olein (PKOlein), and IMEX MCT 60/40 (MCT), containing 60% capric acid and 40% caprylic acid, were supplied by the Malaysian Palm Oil Board (MPOB). The rest of the chemicals used in this study were of analytical grade or equivalent.

Solubility Screening of CXB

An excess amount of CXB was added in 2 ml of single FMCTs oils (PKO, PKOlein, and MCT) and surfactants (Tween 80, Tween 85, Span 80, and Span 20) in a 15 mL capacity screw-capped glass test tube. Mixed FMCTs oils with a ratio of 1:1 (PKO: PKOlein, MCT: PKO, MCT: PKOlein, and PKO:PKOlein: MCT) were also used in the experiment. Each of the samples was mixed using a vortex mixer until homogenized. Then, the samples were equilibrated at 37 ± 2.0°C in an isothermal water bath shaker (Memmerth WNB 22) for 72 h. The equilibrated samples were removed from the shaker and centrifuged at 4000 rpm for 15 min [13]. The supernatant was withdrawn and filtered through a 0.45 µm pore-size membrane filter after being diluted with the necessary amount of ethanol. Spectrophotometric analysis using an ultraviolet-visible (UV-Vis) spectrophotometer (SP-UV200, Perkin Elmer, Shanghai) for CXB in each sample was performed at λ=252 nm against ethanol as blank. All the experiments were performed in triplicate and the results are expressed as mean ± SD.

Determination of HLB Values

The Hydrophilic-Lipophilic Balance (HLB) was employed to calculate the amount of mixed surfactants required for an oil to remain in a solution. The HLB value ranged between 4 to 6 is necessary to form W/O NE while 8 to 18 can form O/W NE. The HLB required for a stable emulsion can be calculated using Equation 1 (14).

$$HLB = (W_a \times HLB_a) + (W_b \times HLB_b)/ W_a + W_b \quad \text{(Equation 1)}$$

W_a represents the amount (weight) of surfactant, W_b shows the amount (weight) of co-surfactant, while HLB_a and HLB_b represent the HLB value of surfactant a and co-surfactant b, respectively.

Construction of Pseudoternary Phase Diagrams

The components (oil, surfactant, and co-surfactant) selected from the solubility studies were utilized for the construction of pseudo-ternary phase diagrams. Primarily, surfactant and co-surfactant were mixed in different weight ratios (1:1, 1:2 and 2:1% w/w) at room temperature to form a mixed surfactant (Smix). Subsequently, individually selected oil phases containing

1% w/w solubilized CXB and each of Smix (1:1, 1:2, and 2:1) were combined in different weight ratios ranging from 0:100 to 100:0, respectively (total weight was 0.5 g). The mixture was then homogenized using a vortex mixer and continuously centrifuged at 4000 rpm for 15 min [15]. Deionized water (5% w/w) was added to each test tube, continuously homogenized, and centrifuged before visual observation was done to determine the physical phase appearance. The transparent or translucent sample was considered an isotropic NE region (Li) while the milky ones until the phase separation layers were formed were considered a multilayer region (M). These steps were repeated with the addition of 10-90% w/w of deionized water [16].

Preparation of CXB-loaded Nanoemulsions

CXB-loaded NE formulations were prepared by using the low energy emulsification method using the phase inversion composition technique, where the aqueous phase was added dropwise into the oil phase. CXB was added into the mixtures of oil, surfactant, and co-surfactant with varying composition ratios (Table 1). The mixture was homogenized using an overhead stirrer (IKA® RW20 Digital, Nara, Japan) at 100 rpm for 15 min. An appropriate amount of deionized water was added dropwise into the mixture while continuously stirring at room temperature to achieve a homogeneous, translucent, and clear NE mixture. All the NEs were stored at room temperature before further analysis.

Thermodynamic Stability Testing

Centrifugation Test

After 15 minutes of centrifugation at 3500 rpm, the formulations were inspected for signs of phase separation, creaming, and cracking. The formulations not showing any phase separation were taken for the heating-cooling cycle [17].

Heating-Cooling Cycle Test

The heating-cooling cycle was performed to investigate how the stability of NE changed in temperature. There were six cycles at each temperature of 4°C and 45°C for no less than 48 h. Then, a cycle of freeze-thaw cycle was performed on stable formulations that were not affected by the temperature tested [18].

Freeze-Thaw Cycle Test

All the prepared formulations were subjected to three cycles of freezing and thawing at the temperatures of -20°C and 25°C at storage temperature for not less than 48 h. Stable formulations were taken for further study [19].

Table 1. The composition of CXB-loaded NE formulations.

NEs	CXB (%w/w)	Oil phase (%w/w)		Smix (%w/w)			Deionized water (%w/w)
		MCT	MCT: PKOlein	1:1	1:2	2:1	
F1	0.04	3.96	-	30	-	-	66
F2	0.03	2.97	-	25	-	-	72
F3	0.02	1.98	-	20	-	-	78
F4	0.04	-	3.96	30	-	-	66
F5	0.03	-	2.97	25	-	-	72
F6	0.02	-	1.98	20	-	-	78
F7	0.04	3.96	-	-	30	-	66
F8	0.03	2.97	-	-	25	-	72
F9	0.02	1.98	-	-	20	-	78
F10	0.04	-	3.96	-	30	-	66
F11	0.03	-	2.97	-	25	-	72
F12	0.02	-	1.98	-	20	-	78
F13	0.04	3.96	-	-	-	30	66
F14	0.03	2.97	-	-	-	25	72
F15	0.02	1.98	-	-	-	20	78
F16	0.04	-	3.96	-	-	30	66
F17	0.03	-	2.97	-	-	25	72
F18	0.02	-	1.98	-	-	20	78

Note: Smix = Tween 80:Tween 85

Preparation of CXB-loaded Nanoemulgels

Carbopol 940 was mixed at 0.5%, 0.75% and 1.0% concentration separately into the water to prepare hydrogel and left overnight to remove any entrapped air. The complete hydrogel was stirred to form a clear gel, and the pH of the hydrogel was adjusted using triethanolamine (TEA). Then, the optimized CXB-loaded NEs were added into the gel base, and stirred for 15 min at 250 rpm using a magnetic stirrer [20, 21].

Characterization of CXB-loaded Nanoemulsion and Nanoemulgel Formulations

Particle Size, Polydispersity Index, and Zeta Potential Measurement

The particle size and polydispersity index (PDI) of NE and NEG formulations were measured by using Zetasizer (Nano ZS, Malvern Instrument Ltd., UK) with dynamic light scattering technique (DLS) at an angle of 90° at room temperature (25 ± 0.5°C). The required number of samples was diluted with deionized water (1:100) before it was injected into the cuvette to make a mean average measurement using intensity distribution. The measurement was repeated in triplicates [17].

For zeta potential analysis, freshly prepared formulations were diluted with deionized water (1:100) and injected into a folded capillary cell (DTS 1070, Malvern Instruments, UK). The measurement was measured at room temperature (25 ± 0.5°C) in triplicates using Zetasizer (Nano ZS, Malvern Instrument Ltd., UK).

pH and Electrical Conductivity Measurements

The pH values of optimized NEs were determined at 25°C using a pH meter (ThermoFisher Scientific Inc., Waltham, MA). Three pH standard buffer solutions (pH 4.01, pH 7.00, pH 10.1) were used for the calibration [20]. Meanwhile, the conductivity of optimized NEs was measured using a conductometer (Mettler Toledo, Switzerland) at room temperature (25 ± 1.0°C) [15].

Morphology Study

The morphology of the droplets of the optimized NEG was studied using Transmission Electron Microscopy (TEM, Tecnai G2 Spirit Bio-Twin, Fei Ltd, Hillsboro, USA). Each of the formulations was diluted 10 times with deionized water and applied on a carbon-coated grid before being allowed to stand for 5 min. Then, a drop of 2% of phosphotungstic acid solution was treated on the grid and dried in the air at room temperature before loading under the microscope for morphological observation [13].

Drug Content

The drug content was determined by dissolving 1.0 g of optimized NEG formulations with ethanol in a centrifuge tube [22]. The resulting sample was kept in a water bath shaker at 37°C for 2 h to solubilize the drug. The sample was then filtered and the absorbance was analyzed using a UV-visible spectrophotometer at 252 nm. The drug content was calculated based on Equation (2) [23].

Drug Content (%) = Analysed drug / Theoretical drug ×100 Equation (3)

Encapsulation Efficiency (EE%)

1.00 g of the optimized NEG formulations were diluted with ethanol in a centrifuge tube and sonicated for 15 min [24]. Then, the samples were centrifuged at 10,000 rpm for 30 min, and the supernatant was collected. The absorbance of the supernatant was filtered and the amount of free drug was measured at 252 nm using UV-visible spectrophotometer against ethanol as a blank. The encapsulation efficiency (EE%) was calculated according to equation (3) [25].

Encapsulation Efficiency (EE %) = [(Total amount of CXB added–free CXB)/ Total amount of CXB added] ×100 Equation (4)

***In Vitro* Drug Release Study**

The *in vitro* drug release study of optimized NE and NEG formulations was carried out using Franz diffusion cells with 0.45 µm cellulose acetate as a diffusional membrane (Sartorius Stedim GmbH, Germany). The volume of the receptor chamber was 5 mL and the diffusion area was 0.64 cm^2. The membrane was mounted between the donor and receptor compartments of Franz diffusion cells. A fresh mixture of the receptor medium containing phosphate buffer solution (PBS): ethanol: Tween 80 of pH 5.5 with a ratio of 79:1:2 was filled in the receptor chamber and stirred at 32°C under continuous stirring at 600 rpm. A total of 1g of the optimized formulations was loaded onto the donor chamber. Samples were withdrawn at specific intervals (15 min, 30 min, 1, 2, 4, 6, 8, 12, and 24 h) and a similar volume of fresh receptor medium was added to maintain sink condition. The drug content of the samples was analyzed using a UV-visible spectroscopy at 252nm. The experiment was performed in triplicate [26].

RESULTS AND DISCUSSION

Solubility Screening of CXB

The solubility of CXB in various oils and surfactants was investigated and presented in Table 2. CXB

exhibited excellent solubilization in MCT (17.43 ± 0.236 mg/ml) followed by its combination with

PKOlein in a 1:1 ratio (14.13 ± 0.128 mg/ml) as compared with other oils and mixed oils. This is due to the polarity of the lipophilic drug that favour its solubility in small or medium molar volume oils like MCT [27]. Furthermore, due to the oleic acid in PKOlein which exhibits a higher partition coefficient of 7.64, it is expected to contribute potent solubilizing capacity for CXB when combined with MCT. Therefore, MCT and mixed oils of MCT: PKOlein (1:1) were selected as the oil phase for the development of the optimal formulation.

In this study, non-ionic surfactants are prioritized as they are generally regarded as safe (GRAS), biocompatible, and less sensitive to pH or ionic strength modifications [28]. Based on the solubility results, CXB showed maximum solubility in Tween 85 (17.64 ± 0.03 mg/ml) and Tween 80 (16.68 ± 0.102 mg/ml) compared to Span 80 and Span 20. The right blend of low and high HLB surfactants leads to the formation of a stable nanoemulsion formulation. Moreover, the surfactant with an HLB value of more than 10 would result in the formation of an O/W type of NE. Therefore, Tween 80 was selected as a surfactant with the HLB value of 15.0 while Tween 85 as the co-surfactant having a low HLB value of 11.0.

Determination of the HLB Values

In this study, Tween 80 and Tween 85 were selected as the surfactant and co-surfactant, respectively, and mixed in varying ratios to form Smix 1:1, 1:2, and 2:1 (%w/w). The HLB values of different Smix ratios were determined in Table 3.

Construction of Pseudoternary Phase Diagrams

In this study, Tween 80 and Tween 85 were mixed in the ratios of 1:1 (%w/w), 1:2 (%w/w), and 2:1 (%w/w), respectively. In Figure 1 (e) and (f), it is noted that the nanoemulsion area (Li region) in both different oils increased substantially when the concentration of Tween 80 used was double in comparison to Tween 85. This confirms to the fact that a higher concentration of surfactant of Tween 80 lowers interfacial tension, increases the fluidity of the interface and thus increases the entropy of the system, resulting in the production of more stable nanoemulsion [29].

Table 2. CXB solubility in various FMCTs oils and surfactants.

Oils	Solubility (mg/ml)	Surfactants	Solubility (mg/ml)
MCT	17.43 ± 0.236	Tween 80	16.68 ± 0.102
PKO	6.89 ± 0.101	Tween 85	17.64 ± 0.03
PKOlein	7.90 ± 0.09	Span 80	7.39 ± 0.566
MCT:PKO (1:1)	10.95 ± 0.114	Span 20	10.73 ± 0.102
MCT:PKOlein (1:1)	14.13 ± 0.128		
PKO:PKOlein (1:1)	7.91 ± 0.09		
MCT:PKO:PKOlein (1:1:1)	9.19 ± 0.06		

Note: Values are expressed as mean ± SD (n=3)

Table 3. The effects of Smix ratio on the HLB value.

Smix Ratio (Tween 80: Tween 85)	HLB Values
1:1	13.00
1:2	12.30
2:1	13.67

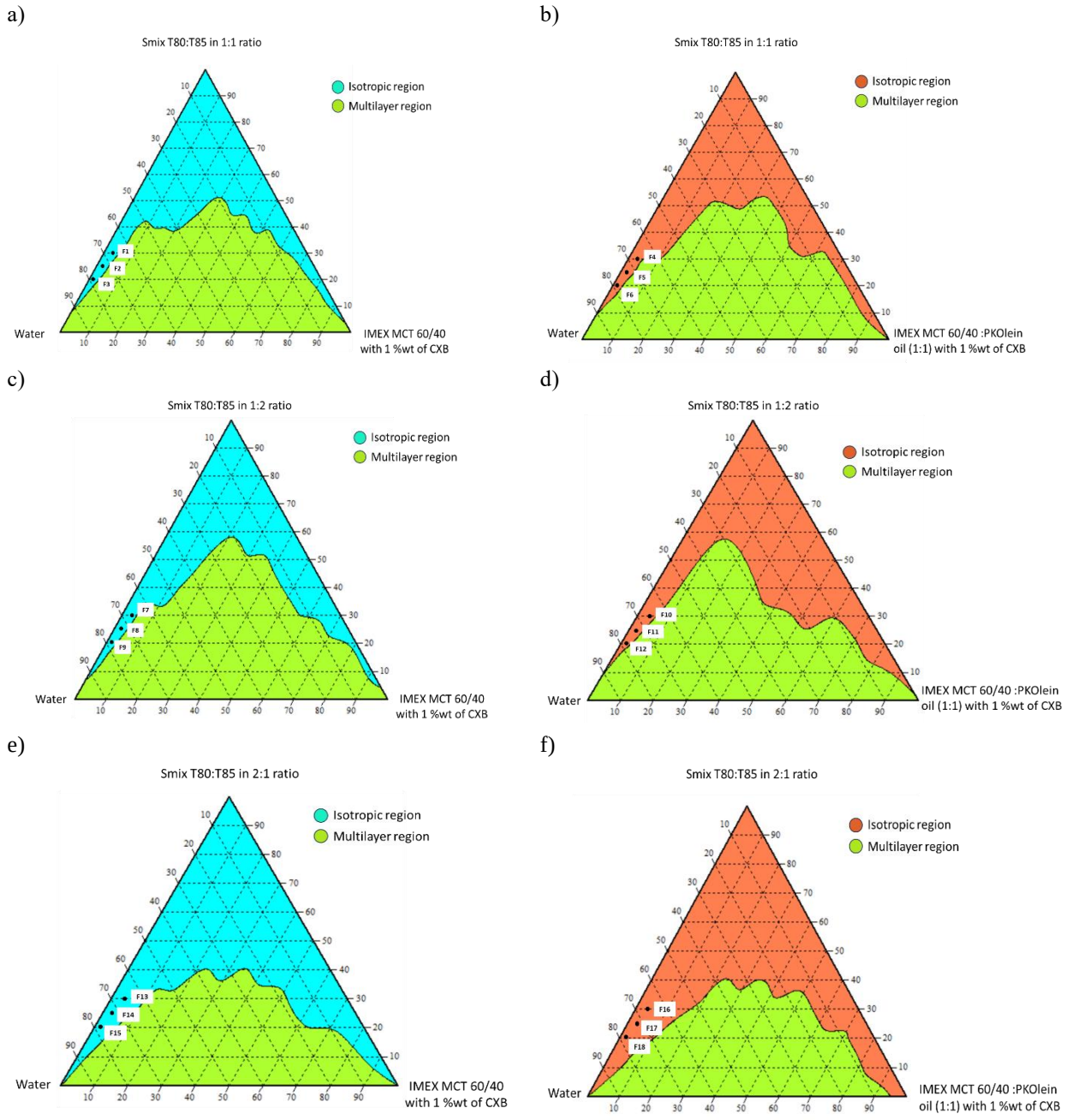

Figure 1. The pseudo ternary phase diagram of selected oil phase at different Smix ratios. F1 to F18 were the formulations selected for the nanoemulsion preparation. Representing (a) MCT with Smix 1:1, (b) MCT: PKOlein (1:1) with Smix 1:1, (c) MCT with Smix 1:2, (d) MCT: PKOlein (1:1) with Smix 1:2, (e) MCT with Smix 2:1, (f) MCT: PKOlein (1:1) with Smix 2:1

After preparing the formulations based on the selected point formula in phase diagrams, the visual observation was recorded in Table 4. NE-F1 to NE-F12 exhibited a milky appearance, indicating the presence of larger particles in the NE. These larger droplets increased multiple scattering, resulting in an opaque or milky aspect [30]. This observation was supported by the Zetasizer particle size analysis, in which the particle size ranged between 114.23 ± 1.021 to 170 ± 1.929 nm (Table 5). In contrast, NE-13 to NE-F18 displayed a clear and translucent appearance due to the smaller particle sizes ranging between 16.87 ± 3.594 to 61.01 ± 1.152 nm (Table 5), which tend to decrease multiple scattering lights, enhancing the transparency of the formulation.

Thermodynamic Stability Testing

NE-F1 to NE-F12 exhibited instability against phase separation, creaming, and cracking, which primarily attributed to their larger particle size. Meanwhile, the stability observed in NE-F13 to NE-F18 can be attributed to the synergistic effects of mixed

surfactants system (Tween 80: Tween 85 in a 2:1 ratio) and the carefully selected ratios of oil, surfactant, and deionized water. Furthermore, the formulations demonstrated relatively small particle sizes as indicated in Table 5. This characteristic serves to prevent flocculation and ensures the absence of phase separation. As a result, the system remains a uniform dispersion, contributing to its stability [31].

Table 4. Thermodynamic stability studies of formulations.

NEs	Physical Appearance	Centrifugation Test	Heating-Cooling Cycle	Freeze-Thaw Cycle	Inferences
F1	Milky	√	X	X	X
F2	Milky	√	X	X	X
F3	Milky	√	X	X	X
F4	Milky	√	X	X	X
F5	Milky	√	X	X	X
F6	Milky	√	X	X	X
F7	Milky	√	X	X	X
F8	Milky	√	X	X	X
F9	Milky	√	X	X	X
F10	Milky	√	X	X	X
F11	Milky	√	X	X	X
F12	Milky	√	X	X	X
F13	Clear/Transparent	√	√	√	√
F14	Clear/Transparent	√	√	√	√
F15	Translucent	√	√	√	√
F16	Clear/Transparent	√	√	√	√
F17	Clear/Transparent	√	√	√	√
F18	Translucent	√	√	√	√

Note: √: Stable (no two layers observed), X: Not stable (two layers observed)

Table 5. Physical appearance, particle size, polydispersity index (PDI), and zeta potential of formulated nanoemulsions.

Formulations	Smix ratio	Composition (%w/w)	Particle Size (nm)*	PDI*	Zeta Potential (mV)*
F1	Tween 80: Tween 85 (1:1)	CXB: 0.04 MCT: 3.96 Smix (1:1): 30 Water: 66	114.23 ± 1.021	0.272 ± 0.011	-12.2 ± 1.513
F2		CXB: 0.03 MCT: 2.97 Smix (1:1): 25 Water: 72	116.47 ± 0.602	0.280 ± 0.010	-15.23 ± 0.057
F3		CXB: 0.02 MCT: 1.98 Smix (1:1): 20 Water: 78	129.1 ± 1.1	0.245± 0.01	-13.9 ± 0.173
F4		CXB: 0.04 MCT:PKOlein (1:1): 3.96 Smix (1:1): 30 Water: 66	119.13 ± 1.939	0.292 ±0.02	-11.23 ± 1.150
F5		CXB: 0.03 MCT:PKOlein (1:1): 2.97 Smix (1:1): 25 Water: 72	119.57 ± 1.209	0.267 ± 0.01	-12.87 ± 1.365

F6		CXB: 0.02 MCT:PKOlein (1:1): 1.98 Smix (1:1): 20 Water: 78	126.97 ± 1.201	0.252 ± 0.01	-15.13 ± 0.513
F7	Tween 80: Tween 85 (1:2)	CXB: 0.04 MCT: 3.96 Smix (1:2): 30 Water: 66	131.1 ± 0.964	0.252 ± 0.01	-20.2 ± 3.67
F8		CXB: 0.03 MCT: 2.97 Smix (1:2): 25 Water: 72	151.17 ± 1.530	0.241 ± 0.00	-17.87 ± 0.152
F9		CXB: 0.02 MCT: 1.98 Smix (1:2): 20 Water: 78	147.9 ± 0.608	0.237 ± 0.01	-18.57 ± 0.802
F10		CXB: 0.04 MCT:PKOlein (1:1): 3.96 Smix (1:2): 30 Water: 66	158.3 ± 0.458	0.226 ± 0.01	-21.4 ± 1.374
F11		CXB: 0.03 MCT:PKOlein (1:1): 2.97 Smix (1:2): 25 Water: 72	132. 1 ± 0.435	0.231 ± 0.01	-17.23 ± 0.750
F12		CXB: 0.02 MCT:PKOlein (1:1): 1.98 Smix (1:2): 20 Water: 78	170 ± 1.929	0.234 ± 0.01	-17.3 ± 0.871
F13	Tween 80: Tween 85 (2:1)	CXB: 0.04 MCT: 3.96 Smix (2:1): 30 Water: 66	24.67 ± 4.284	0.370 ± 0.08	-20.37 ± 6.406
F14		CXB: 0.03 MCT: 2.97 Smix (2:1): 25 Water: 72	21.89 ± 0.199	0.467 ± 0.05	-17.7 ± 3.629
F15		CXB: 0.02 MCT: 1.98 Smix (2:1): 20 Water: 78	61.01 ± 1.152	0.526 ± 0.01	-12.13 ± 2.079
F16		CXB: 0.04 MCT:PKOlein (1:1): 3.96 Smix (2:1): 30 Water: 66	18.26 ± 2.102	0.330 ± 0.075	-13.93 ± 3.332
F17		CXB: 0.03 MCT:PKOlein (1:1): 2.97 Smix (2:1): 25 Water: 72	16.87 ± 3.594	0.379 ± 0.01	-16.93 ± 3.564
F18		CXB: 0.02 MCT:PKOlein (1:1): 1.98 Smix (2:1): 20 Water: 78	54.75 ± 1.426	0.524 ± 0.03	-16.23 ± 6.404

*Values are expressed as mean ± SD (n=3).

Characterization of the CXB-loaded Nanoemulsions and Nanoemulgels

Particle Size, Polydispersity Index (PDI), Zeta Potential, pH, and Conductivity Analysis

The average droplet size of the prepared NE lay in the nanosized range between 16.87± 3.594 to 170 ± 1.929 nm (Table 5) as required for the NE formulation (20-200 nm). It has been reported earlier that the smaller the size of NE droplets, the faster the drug permeation through the skin layers. It helps to facilitate easier permeation through several layered skin structures and provides greater surface area for faster drug release [13]. According to this study, NE-F14 (21.89 ± 0.199 nm) and NE-F17 (16.87 ± 3.594 nm) demonstrated the smallest particle sizes among the different oils used, namely the MCT oil and MCT: PKOlein (1:1) oil, respectively. It appeared that medium total chain lengths facilitated the formation of a smaller droplet size, as shown in MCT oil [32]. On top of that, when combined with PKOlein in a 1:1 ratio, the high concentrations of lauric acid and oleic acid in PKOlein decreased the interfacial tension that led to a smaller particle size. Higher conductivity values in NE-F14 and NE-F17 (Table 6), with 244.0 ± 1.000 µS/cm and 188.132 ± 0.153 µS/cm, respectively, confirmed the O/W NE types [33].

Due to their small particle size, NE-F14 and NE-F17 were selected as the optimum formulations. Subsequently, these formulations were further characterized and modified into NEGs with varying concentrations (0.5%, 0.75%, and 1.0% w/w). Based on the results shown in Table 7, all NEGs with varied concentrations produced larger sizes compared to their respective NE formulations. In addition, the increase in Carbopol 940 concentration (0.5%, 0.75%, and 1.0% w/w) led to an enlargement of droplet sizes within the nanosized range in both NEG-F14 and NEG-F17. Similar outcomes were also reported by Eid et al. [34], who noted that the addition of the polymer Carbopol increased the viscosity of the medium due to the high degree of cross-linking in the gel, resulting in larger particle sizes.

Low PDI (below 0.7) observed in the NE and NEG formulations of F14 and F17 (Table 6 and Table 7, respectively) indicates that the samples had uniform distribution, high quality, and homogeneity of nanosized droplets [19]. However, the zeta potential in NE formulations of F14 and F17 was less than -30mV. This could be due to the greater steric effect that resulted in less electrostatic stabilization upon the addition of non-ionic surfactants such as Tween 80 and Tween 85 [35]. In contrast to NEGs, the zeta potential became more negative and this suggested that the NEG had a relatively good stability after the addition of Carbopol gel. This shift in zeta potential indicated an influence on the surface charge of the droplets.

According to Eid et al. [34], the addition of 0.5% Carbopol 940 is preferred as a thickening agent because it has ideal viscosity and rheological behaviour as compared to 0.75% and 1.0% Carbopol 940. Therefore, NEG-F14 and NEG-F17 with 0.5% Carbopol 940 were chosen as optimized NEG formulations for further study. Moreover, the pH of all the NE and NEG of F14 and F17 falls within the optimal range of human skin pH (4.5 – 6.6), which is suitable for topical and transdermal applications, signifies the absence of skin irritancy (Table 6 and Table 7) [36].

Table 6. pH and electrical conductivity of optimal NE formulations (NE-F14 and NE-F17).

Formulations	pH*	Conductivity, µS/cm*
NE-F14	6.319 ± 0.002	244.0 ± 1.000
NE-F17	6.333 ± 0.003	188.132 ± 0.153

*Values are expressed as mean ± SD (n=3).

Table 7. Particle size, polydispersity index (PDI) and zeta potential of NEG.

Formulations	Concentration of Carbopol 940 (%w/w)	Particle Size (nm)*	PDI*	Zeta Potential (mV)*	pH*
NEG-F14	0.5	26.75 ± 6.105	0.377 ± 0.061	-24.17 ± 3.324	6.52 ± 0.002
	0.75	41.30 ± 4.085	0.231 ± 0.046	-22.47 ± 1.650	6.42 ± 0.004
	1.0	53.47 ± 5.349	0.213 ± 0.022	-26.03 ± 0.981	6.19 ± 0.019
NEG-F17	0.5	26.85 ± 0.661	0.488 ± 0.012	-38.83 ± 7.600	6.52 ± 0.002
	0.75	40.81 ± 3.938	0.177 ±0.014	-36.07 ± 1.150	6.45 ± 0.010
	1.0	55.87 ± 3.496	0.272 ± 0.043	-25.87 ± 3.855	6.43 ± 0.010

Note: *Values are expressed as mean ± SD (n=3).

a) b)

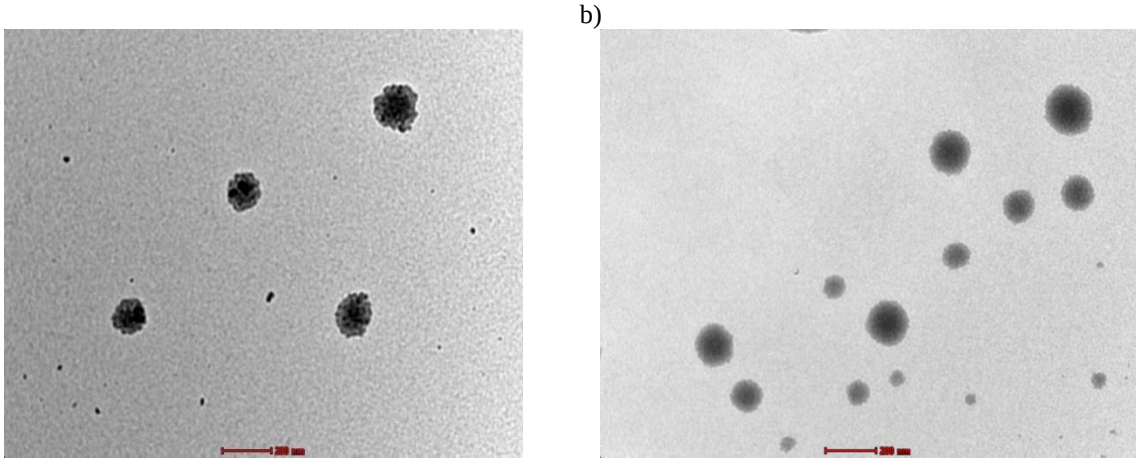

Figure 2. The TEM images of the optimized formulations (a) CXB-loaded NEG F14 0.5% Carbopol 940 and (b) CXB-loaded NEG F17 0.5% Carbopol 940.

Morphology Analysis

Figure 2 shows that the droplets of both the selected formulations are spherical and their size are within the nanoscale range of ≤200 nm, which agrees with the results obtained from the Zetasizer equipment.

Drug Content and Encapsulation Efficiency

The optimized formulations of NEG-F17 0.5% Carbopol 940 had the higher drug content (97.54 %) with 83.39 % of EE when compared with NEG-F14 0.5% Carbopol 940 (Table 8). This might be due to the presence of palm kernel olein in nanoemulsion that improve the solubility, where oils with a higher molecular mass reduced water solubility, inhibited Ostwald ripening and providing emulsion stability [37], thus increasing the drug solubility.

***In Vitro* Drug Release Study**

The *in vitro* release studies were conducted using Franz diffusion cells to compare the release pattern of CXB between different NEG formulations.

Table 8. Drug content and encapsulation efficiency of optimized NEGs formulations.

Formulations	Drug content (%) *	Encapsulation Efficiency (%) *
NEG-F14 0.5% Carbopol 940	94.03 ± 0.079	82.22 ± 0.169
NEG-F17 0.5% Carbopol 940	97.54 ± 0.072	83.39 ± 0.399

Note: *Values are expressed as mean ± SD (n=3).

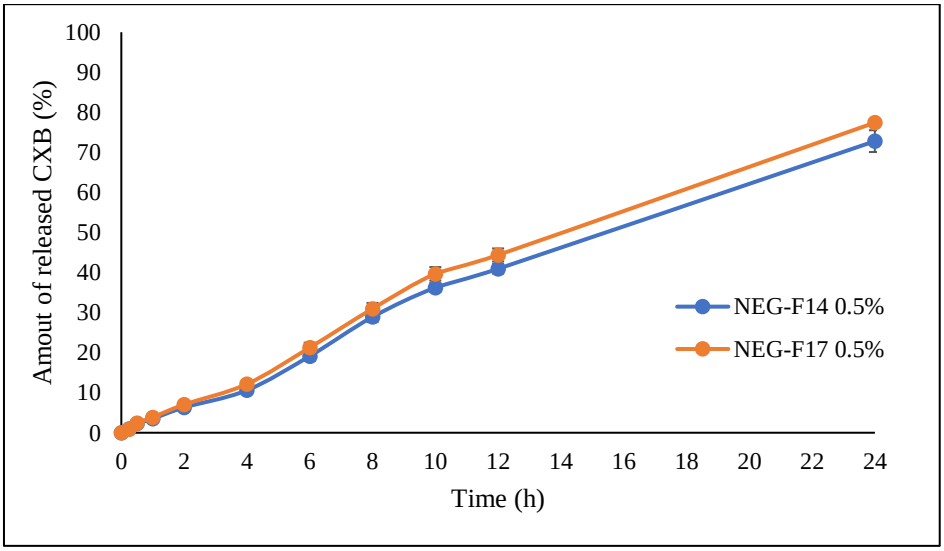

Figure 3. Release profiles of CXB from NEG-F14 and NEG-F17 containing 0.5% Carbopol 940.

In 24 h, the release of CXB from NEG-F17 0.5% Carbopol 940 was remarkably higher (77.60 ± 1.41%) as compared to NEG-F14 0.5% Carbopol 940 (72.85 ± 0.93%) even though both had smaller particle sizes (Figure 3). This might be attributed to the presence of a mixture between the medium and long-chain triglycerides (caprylic, capric, lauric and oleic acid) in MCT:PKOlein oil, which further enhanced the dispersion rate of oil droplets containing CXB to travel quickly to reach the release medium, resulting in a higher drug release in NEG-F17 0.5% Carbopol 940. Nonetheless, these did not adversely hinder drug release, where more than 70% of the loaded drug was released from different gel formulations at 24 h, thereby ensuring effective and sustained drug permeation potential for transdermal delivery.

CONCLUSION

In this study, based on the characterization studies including particle size, polydispersity index (PDI), and zeta potential assessments, NE-F14 using MCT and NE-F17 using MCT:PKOlein (1:1) as the oil phase were confirmed as the optimal formulations for further development. These formulations demonstrated the smallest particle size, low PdI, and acceptable zeta potential values, indicating a good stability. The resulting optimized CXB-loaded NEGs also maintained smaller nano-droplets size with a uniform distribution under TEM, showing the maximum drug content and encapsulation efficiency (<80%) as well as higher drug release rate with more than 70%, thereby ensuring its potential in transdermal delivery. To sum up, the developed NEGs might be a promising approach to improve the poorly permeable CXB for transdermal delivery.

ACKNOWLEDGEMENTS

We would like to thank the Ministry of Higher Education, Malaysia, for the provision of a research grant under the Fundamental Research Grant Scheme (FRGS) (FRGS/1/2021/STG04/UITM/02/8). Special thanks to the Faculty of Pharmacy, Universiti Teknologi MARA for all the resources provided throughout this project.

REFERENCES

1. Turk, M. J., Breur, G. J., Widmer, W. R., Paulos, C. M., Xu, L. C., Grote, L. A. and Philip, S. L. (2002) Folate-targeted imaging of activated macrophages in rats with adjuvant-induced arthritis. *Arthritis & Rheumatology*, **46(7)**, 1947–1955.

2. Cheng, T., Tai, Z., Shen, M., Li, Y., Yu, J., Wang, J., Zhu, Q. and Chen, Z. (2023) Advance and Challenges in the Treatment of Skin Diseases with the Transdermal Drug Delivery System. *Pharmaceutics*, **15(8)**, 2165.

3. Tadros, T., Izquierdo, P., Esquena, J. and Solans, C. (2004) Formation and stability of nano-emulsions. *Advances in Colloid and Interface Science*, **108–109**, 303–318.

4. Sengupta, P. and Chatterjee, B. (2017) Potential and future scope of nanoemulgel formulation for topical delivery of lipophilic drugs. *International Journal of Pharmaceutics*, **526(1–2)**, 353–365.

5. Pawar, K. R. and Babu, R. J. (2014) Lipid materials for topical and transdermal delivery of nanoemulsions. *Critical Reviews in Therapeutic Drug Carrier System*, **31(5)**, 429–458.

6. Inthiram, A. K., Mirhosseini, H., Tan, C. P., Mohamad, R. and Lai, O. M. (2015) Application of multivariate analysis for detection of crude palm oil adulteration through fatty acid composition and Triacylglycerol profile. *Pertanika Journal of Tropical Agricultural Science*, **38(3)**, 389–398.

7. Ghazani, S. M. and Marangoni, A. G. (2020) Fractionated coconut oil and MCT oil production: Facts and fiction. *INFORM-International News on Fat*, **31(9)**, 29–32.

8. Shaikh, A. A., Swami, V., Buchade, R. S. and Jadhav, P. N. (2021) Formulation Development of Celecoxib Loaded Microsponges using Eudragit and Ethyl Cellulose. *International Journal of Pharmaceutical Investigation*, **11(2)**, 225–229.

9. Crofford, L. J. (2013) Use of NSAIDs in treating patients with arthritis. *Arthritis Research and Therapy*, **15(3)**, S2.

10. Reddy, M. N., Rehana, T., Ramakrishna, S., Chowdary, K. P. R. and Diwan, P. V. (2004) β-cyclodextrin complexes of celecoxib: Molecular-modeling, characterization, and dissolution studies. *American Association of Pharmaceutical Scientists*, **6(1)**, 68–76.

11. RxList (2022) Celebrex (Celecoxib): Uses, Dosage, Side Effects, Interactions.

12. Shakeel, F. and Faisal, M. S. (2010) Nanoemulsion: A promising tool for solubility and dissolution enhancement of celecoxib. *Pharmaceutical Development and Technology*, **15(1)**, 53–56.

13. Kaur, R. and Ajitha, M. (2019) Transdermal delivery of fluvastatin loaded nanoemulsion gel: Preparation, characterization and *in vivo* anti-osteoporosis activity. *European Journal of Pharmaceutical Sciences*, **136**, 1–10.

14. Ullah, N., Amin, A., Farid, A., Selim, S., Rashid, S. A., Aziz, M. I., Kamran, S. H., Khan, M. A., Khan, N. R, Mashal, S. and Hasan, M. M. (2023) Development and Evaluation of Essential Oil-Based Nanoemulgel Formulation for the Treatment

of Oral Bacterial Infections. *Gels*, **9(3)**, 1–21.

15. Thuraisingam, S., Salim, N., Azmi, I. D. M., Kassim, N. K. and Basri, H. (2023) Development of Nanoemulsion containing *Centella Asiatica* Crude Extract as a Promising Drug Delivery System for Epilepsy Treatment. *Biointerface Research in Applied Chemistry*, **13(1)**, 1–24.

16. Salim, N., Basri, M., Rahman, M. B. A., Abdullah, D. K., Basri, H. and Salleh, A. B. (2011) Phase behavior, formation and characterization of palm-based esters nanoemulsion formulation containing ibuprofen. *Journal of Nanomedicine Nanotechnology*, **2(4)**, 1–5.

17. Al Fatease, A., Alqahtani, A., Khan, B. A., Mohamed, J. M. M. and Farhana, S. A. (2023) Preparation and characterization of a curcumin nanoemulsion gel for the effective treatment of mycoses. *Scientific Reports*, **13(1)**, 22730.

18. Yeo, E., Chieng, C. J. Y., Choudhury, H., Pandey, M. and Gorain, B. (2021) Tocotrienols-rich naringenin nanoemulgel for the management of diabetic wound: Fabrication, characterization and comparative *in vitro* evaluations. *Current Research in Pharmacology and Drug Discovery*, **2(100019)**, 1–10.

19. Fadhel, A. Y. and Rajab, N. A. (2022) Tizanidine Nanoemulsion: Formulation and *in-vitro* Characterization. *Journal of Pharmaceutical Negative Results*, **13(3)**, 572–581.

20. Rashid, S. A., Bashir, S., Naseem, F., Farid, A., Rather, I. A. and Hakeem, K. R. (2021) Olive oil based methotrexate loaded topical nanoemulsion gel for the treatment of imiquimod induced psoriasis-like skin inflammation in an animal model. *Biology (Basel)*, **10(11)**, 1121.

21. Naeem, M., Iqbal T., Nawaz Z. and Hussain, S. (2021) Preparation, optimization and evaluation of transdermal therapeutic system of celecoxib to treat inflammation for treatment of rheumatoid arthritis. *Anais da Academia Brasileira de Ciências*, **93(4)**, 93, e20201561.

22. Sharma, B., Iqbal, B., Kumar, S., Ali, J. and Baboota, S. (2019) Resveratrol-loaded nano-emulsion gel system to ameliorate UV-induced oxidative skin damage: from *in vitro* to *in vivo* investigation of antioxidant activity enhancement. *Archives of Dermatological* Research, **311(10)**, 773–793.

23. Ashoor, J. A. and Ghareeb, M. M. (2022) Formulation and *In-vitro* Evaluation of Methotrexate Nanoemulsion using Natural Oil. *International Journal of Drug Delivery Technology*, **12(2)**, 670–677.

24. Alshehri, S., Bukhari, S. I., Imam, S. S., Hussain, A., Alghaith, A. F., Altamimi, M. A., AlAbdulkarim, A. and Almurshedi, A. (2023) Formulation of Piperine-Loaded Nanoemulsion: *In Vitro* Characterization, Ex Vivo Evaluation, and Cell Viability Assessment. *American Chemical Society Omega*, **8(25)**, 22406–22413.

25. Abdellatif, A. A. H., Ali, A. T., Bouazzaoui, A., Alsharidah, M., Al Rugaie, O. and Tolba, N. S. (2022) Formulation of polymeric nanoparticles loaded sorafenib; Evaluation of cytotoxicity, molecular evaluation, and gene expression studies in lung and breast cancer cell lines. *Nano-technology Reviews*, **11(1)**, 987–1004.

26. Kaplan, U. A. B., Cetin, M., Orgul, D., Taghizadehghalehjoughi, A., Hacımuftuoglu, A. and Hekimoglu, S. (2019) Formulation and *in vitro* evaluation of topical nanoemulsion and nanoemulsion-based gels containing daidzein. *Journal of Drug Delivery Science Technolology*, **52**, 189–203.

27. Gaba, B., Khan, T., Haider, M. F., Alam, T., Baboota, S., Parvez, S. and Ali, J. (2019) Vitamin E Loaded Naringenin Nanoemulsion via Intranasal Delivery for the Management of Oxidative Stress in a 6-OHDA Parkinson's Disease Model. *Biomed Research International*, 2019, **2382563**, 1–20.

28. Azeem, A., Rizwan, M., Ahmad, F. J., Iqbal, Z., Khar, R. K., Aqil, M. and Talegaonkar, S. (2009) Nanoemulsion components screening and selection: A technical note. *American Association of Pharmaceutical* Scientists, **10(1)**, 69–76.

29. Baboota, S., Shakeel, F., Ahuja, A., Ali, J. and Shafiq, S. (2007) Design, development, and evaluation of novel nanoemulsion formulations for transdermal potential of celecoxib. *Acta Pharmaceutica*, **57(3)**, 315–332.

30. Molet-Rodríguez, A., Salvia-Trujillo, L. and Martín-Belloso, O. (2018) Beverage emulsions: Key aspects of their formulation and physicochemical stability. *Beverages*, **4(3)**, 70.

31. Izadiyan, Z., Basri, M., Masoumi, H. R. F., Abedi, R. K., Salim, N. and Shameli, K. (2017) Modeling and optimization of nanoemulsion containing Sorafenib for cancer treatment by response surface methodology. *Chemistry Central Journal*, **11(1)**, 21.

27. Weerapol, Y., Manmuan, S., Chaothanaphat, N., Okonogi, S., Limmatvapirat, C., Limmatvapirat, S. and Tubtimsri, S. (2022) Impact of Fixed Oil on Ostwald Ripening of Anti-Oral Cancer Nano-emulsions Loaded with *Amomum kravanh* Essential Oil. *Pharmaceutics*, **14(5)**, 938.

32. Sarheed, O., Dibi, M. and Ramesh, K. V. R. N. S.

(2020) Studies on the effect of oil and surfactant on the formation of alginate-based O/W lidocaine nanocarriers using nanoemulsion template. *Pharmaceutics*, **12(12)**, 1–21.

33. Ribeiro, R. C. D. A., Barreto, S. M. A. G., Ostrosky, E. A., Da Rocha-Filho, P. A, Veríssimo, L. M. and Ferrari, M. (2015) Production and characterization of cosmetic nanoemulsions containing *Opuntia ficus-indica* (L.) Mill extract as moisturizing agent. *Molecules*, **20(2)**, 2492–2509.

34. Eid, A. M., El-Enshasy, H. A., Aziz, R. and Elmarzugi, N. A. (2014) Preparation, characterization and anti-inflammatory activity of *Swietenia macrophylla* nanoemulgel. *Journal of Nanomedicine & Nanotechnology*, **5(2)**, 1–10.

35. Bhakay, A., Rahman, M., Dave, R. N. and Bilgili, E. (2018) Bioavailability Enhancement of Poorly Water-Soluble Drugs via Nanocomposites: Formulation–Processing Aspects and Challenges. *Pharmaceutics*, **10(3)**, 86.

36. Banerjee, S., Chattopadhyay, P., Ghosh, A., Bhattacharya, S. S., Kundu, A. and Veer, V. (2014) Accelerated stability testing of a transdermal patch composed of eserine and pralidoxime chloride for prophylaxis against (±)-anatoxin a poisoning. *Journal of Food and Drug Analysis*, **22(2)**, 264–270.

37. Ahmed, K., Li, Y., McClements, D. J. and Xiao, H. (2012) Nanoemulsion- and emulsion-based delivery systems for curcumin: Encapsulation and release properties. *Food Chemistry*, **132(2)**, 799–807.